Photonic crystal modulator in a CMOS foundry platform

Kenaish Al Qubaisi^{1,*}, Deniz Onural¹, Hayk Gevorgyan¹, and Miloš A. Popović^{1,†}

¹Department of Electrical and Computer Engineering, Boston University, Boston, MA 02215, USA

*kalqubai@bu.edu, †mpopovic@bu.edu

Abstract: We report the first photonic crystal microcavity modulator realized in a foundry CMOS photonics platform. Bandwidth of 2.8 GHz and 5 Gbps data rate demonstrated utilizing an interdigitated p-n junction in a WDM compatible structure. © 2021 The Author(s)

Photonic crystals give the smallest mode volumes and most compact footprint among dielectric photonic microcavities [1]. The could enable the ultimate efficiencies in active devices like modulators and photodiodes, as well as whole links - and potentially enable receiverless links [2]. Yet, utilizing photonic crystals (PhC) to implement modulators or detectors, in integrated wavelength division multiplexing (WDM) optical links has long been overlooked in favor of microring resonators. This has two main reasons. The first is the demanding nature of photonic crystal devices in terms of fabrication capabilities. The high lithography resolution required to define the structure and the small feature size required to implement the doping implants rule out almost all of the standard silicon-on-insulator (SOI) photonic platforms as viable options to realize such devices. And, although electron-beam (e-beam) lithography platforms capable of realizing active devices do exist, they have provide very crude and large doping patterns [3, 4], which are unfit for realizing advanced p-n junction designs such as interdigitated junctions [5]. In addition, e-beam lithography is not practical for manufacturing photonic systems with large number of components. The second reason for choosing microring reosnators for WDM system components over PhC nanobeam cavities has been the standing-wave nature of the latter. This means that when light is coupled evanescently to a PhC nanobeam microcavity via a bus waveguide, a portion of the light is reflected back into the bus waveguide, which is highly undesirable in WDM systems [6].

These two reasons are not entirely uncorrelated. For instance, if one is to design a PhC nanobeam modulator that side-couples light evanescently from a bus on one side, as is the case with microring modulators, then the designer is forced to place contacts on the opposite side. Moreover, the designer is left with two options for the design of a *p-n* junction, either an interdigitated junction or a vertical junction [7], both requiring advanced fabrication capabilities. For this reason, and to the best of our knowledge, in all of the proposed PhC active devices in silicon photonics, light is always butt-coupled into the cavity and either a horizontal *p-n* junction [8, 9] or a *p-i-n* diode [3, 4, 10, 11] is implemented. Such a coupling mechanism is undesirable in WDM systems since it yields a structure which is not transparent to other channels, thus reflecting all channels outside the transmission band of the PhC modulator. This significantly complicates any WDM system design which seeks to utilize PhC based devices, as it requires either complex interferometers or circulators.

A new generation 45 nm-node photonics-tailored electronics-photonics platform, GlobalFoundries 45CLO [12], supports high resolution lithography and multiple small-feature size doping implant layers, allowing for devices with fine features and complex *p-n* junction designs. This process goes beyond the 45 nm-node electronic-photonic platform (IBM 12SOI/GF 45RFSOI [13]) used to demonstrate complex systems like the first microprocessor with monolithically integrated optical I/O [14], in that it uses the same base transistors but optimizes photonics. Moreover, we recently proposed and demonstrated (also in the 45CLO process) a novel architecture allowing for seamless integration of PhC nanobeam cavities in WDM systems [6] resolving the standing-wave issue. This allows designers to harness the excellent light confining capabilities of PhC nanobeam cavities [1] in order to realize ultra-low energy and compact active devices.

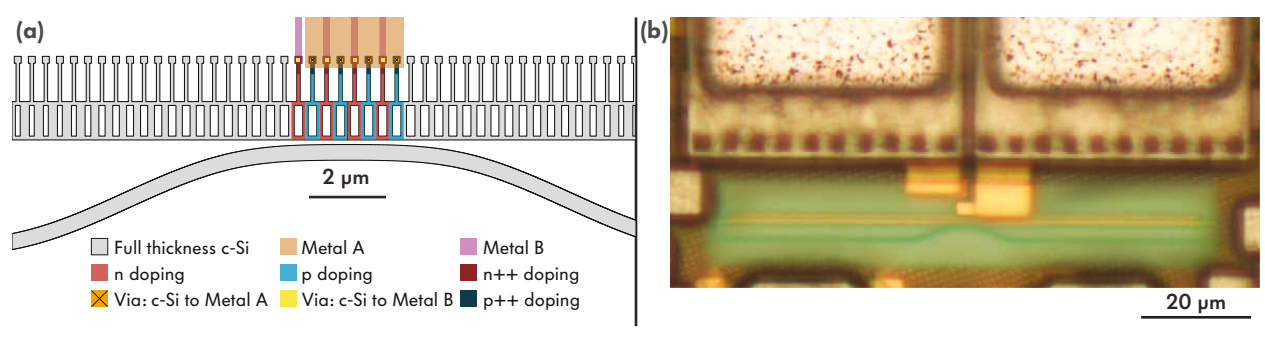


Fig. 1: (a) Geometry of the PhC nanobeam cavity modulator as laid out on the design mask. (b) Optical micrograph of the device.

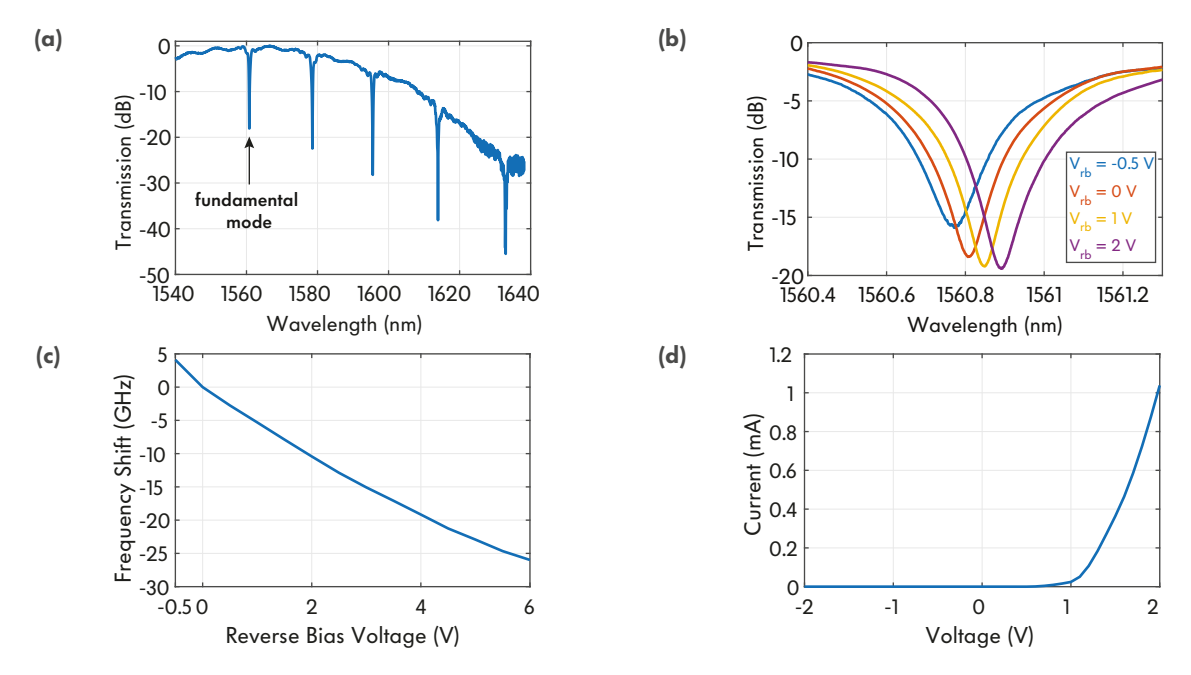


Fig. 2: (a) Wide spectra of the transmission response with the fundamental resonance mode indicated. (b) Resonant optical response at DC bias voltages from -2 to 0.5 V. (c) Resonance frequency shift as a function of applied voltage. (d) I-V curve of the PhC nanobeam modulator.

In this paper, we report the first demonstration of a PhC modulator in a CMOS foundry platform. Moreover, owing to the sub-wavelength contacts placed on one side of the cavity and the interdigitated *p-n* junction, this is also the first demonstration of a PhC nanobeam cavity modulator where light is coupled evanescently into the cavity via a bus waveguide. This makes the structure compatible with trivial WDM cascading, akin to microring modulators [15], when implemented in the previously mentioned architecture [6]. The proposed device is illustrated in Fig. 1(a) and an optical micrograph of the PhC nanobeam cavity modulator showing the termination pads is shown in Fig. 1(b).

The PhC nanobeam cavity modulator was designed using the approach presented in [1] to operate in the C-band, near 1550 nm, and to support the dielectric-mode. The waveguide width of the PhC nanobeam cavity was set to $1 \mu m$ and the period of the low-index etch holes to 344 nm. The low-index etch holes were implemented by etching 800 nm wide rectangular holes across the waveguide width and the mirror strength was varied by varying their duty cycle along the length. The mirror strength was increased linearly over 20 periods on each side of the cavity, with many more uniform mirror holes added on each side. However, ten mirror holes on each side were sufficient to achieve an intrinsic quality factor exceeding 200k in the same process [6]. The length of the sub-wavelength contacts was set to 1.18 μm with a width of 90 nm. The contacts are placed at the nodes of the fundamental longitudinal resonance mode of the cavity [10].

In the current implementation, the gap between the bus waveguide and the PhC nanobeam cavity was set to 270 nm, such that the cavity is over-coupled to the bus waveguide resulting in a large extinction ratio in the transmission response [6]. However, this comes at a cost of widening the cavity's linewidth and reducing the optical modulation amplitude (OMA) of the device. When implementing a WDM compatible architecture using this modulator, a larger gap will be used in order to achieve near critical coupling [6], thus reducing the linewidth of the cavity and improving the OMA of the modulator. A wide spectrum is shown in Fig. 2(a), showing the fundamental resonance mode at 1560.8 nm with an extinction >17 dB and an approximate linewidth of 75 GHz, in addition to the high-order resonance modes. The free-spectral range (FSR) between the fundamental mode and the first-order mode was measured to be 2.16 THz.

Four periods were doped on each side of the cavity with alternating doping implants in order to realize an interdigitated junction and achieve modulation. We estimate that the capacitance of the device is 1.9 fF. This is smaller by at least a factor of seven when compared to the device in [7] which holds the record for energy-per-bit figure of merit among silicon photonic modulators. The DC response of the modulator is shown in Fig. 2(b-c). The shift efficiency was measured to be 5.3 GHz/V.

The electro-optical bandwidth of the modulator with 0 V applied at the terminals is shown in Fig. 3(a), showing

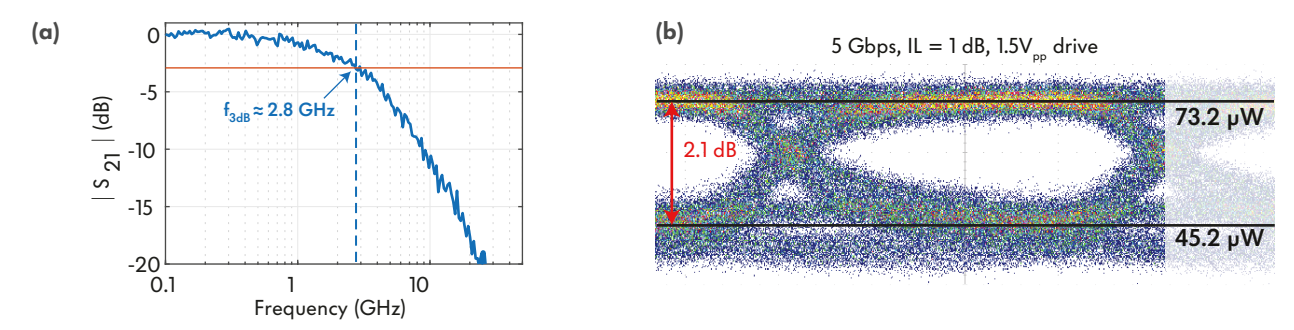


Fig. 3: (a) Electro-optic response frequency response of the modulator with 0 V applied at the terminals. (b) 5 Gbps optical eye diagram with 2.1 dB modulation depth and insertion loss of 1 dB in response to voltage swing from -1.75 V to 0.25 V applied at the terminals.

bandwidth of 2.8 GHz. Comparing the measured bandwidth to the measured resonance linewidth clearly indicates that the bandwidth is RC limited. Using the estimated device capacitance and measured bandwidth, we estimate that the device resistance is 29.8 k Ω . The large resistance is mainly due to the long and narrow path between the middle of the p-n junction and end of the contacts. Measured optical eye diagram of the PhC nanobeam modulator fed by a non-return-to-zero (NRZ) PRBS7 signal, indicating insertion loss and extinction ratio, is shown in Fig. 3(b). The voltage waveform of 1.5V_{pp} driving the modulator does not include the up to $2\times$ reflection-induced voltage bump due to the capacitive device impedance. Even with that, the device remains in depletion mode operation. We can estimate the energy-per-bit of the device using the equation $E_b = \frac{1}{4}CV_{pp}^2$, resulting in an energy-per-bit of 1 fJ/bit. Although it is yet to be measured and confirmed experimentally, this is on par with the lowest energy-per-bit (0.9 fJ/bit) demonstrated to date [7] using a microring modualtor but with a more efficient vertical junction.

In conclusion, we demonstrated the first PhC nanobeam microrcavity modulator in a CMOS platform with 5 Gbps operation, 2.16 THz FSR, and ultra-low estimated energy-per-bit of 1 fJ/bit. Moreover, this is also the first PhC based active device which is straightforward to cascade into a WDM architecture. Such demonstration in a 45 nm CMOS monolithic platform paves the path for new integrated systems-on-chip with a next level of performance in terms of footprint, bandwidth density, and energy consumption.

Acknowledgments: We thank the GlobalFoundries 45CLO process team and Ayar Labs, Inc. for extensive support and interaction. Fabricated on the Pico test vehicle. Funding: National Science Foundation Award #2023751 (ASCENT), ODNI/IARPA via U.S. ARO grant W911NF-19-2-0114 (SuperCables), and a fellowship from the Abu Dhabi National Oil Company.

References

- 1. Q. Quan, et al. "Deterministic design of wavelength scale, ultra-high Q ..." Opt. Express 19.19 (2011): 18529-18542.
- 2. D. Miller, "Attojoule optoelectronics for low-energy information processing ..." JLT 35.3 (2017): 346-396.
- 3. B. Schmidt, et al., "Compact electro-optic modulator on silicon-on-insulator substrates ..." Opt. Express 15.6, (2007): 3140-3148.
- 4. A. Shakoor, et al., "Compact 1D-silicon photonic crystal electro-optic modulator ..." Opt. Express 22.23, (2014): 28623-28634.
- 5. J.M. Shainline, et al., "Depletion-mode carrier-plasma optical modulator in zero-change..." Opt. Lett. 38.15, (2013): 2657-2659.
- 6. K. Al Qubaisi, et al., "Reflectionless dual standing-wave microcavity resonator units..." Opt. Express 28.24, (2020): 35986-35996.
- 7. E. Timurdogan, et al., "An ultralow power athermal silicon modulator" Nature Communications 5.1, (2014): 1-11.
- 8. J. Hendrickson, et al., "Ultrasensitive silicon photonic-crystal nanobeam electro-optical ..." Opt. Express 22.3 (2014): 3271-3283.
- 9. M. Caverley, et al., "Silicon-on-insulator modulators using a quarter-wave ..." IEEE Photon. Technol. Lett. 22.3 27.22 (2015): 2331-2334.
- 10. S. Meister, et al., "Matching pin-junctions and optical modes enables fast and ultra-small ..." Opt. Express 21.13 (2013): 16210-16221.
- 11. K. Mehta, et al., "High-Q CMOS-integrated photonic crystal microcavity devices." Sci. Rep 4.1 (2014): 1-6.
- 12. M. Rakowski, et al., "45nm CMOS Silicon Photonics Monolithic Technology (45CLO) ..." OFC, OSA, paper T3H.3 (2020).
- 13. V. Stojanović, R. J. Ram, M. Popović, S. Lin, S. Moazeni, M. Wade, C. Sun, et al., Opt. Express. 26, 13106–13121 (2018).
- 14. C. Sun, M. T. Wade, et al., "Single-chip microprocessor that communicates directly using light." Nature 528, 534-538 (2015).
- 15. M. Wade et al., "TeraPHY: A Chiplet Technology for Low-Power, High-BW In-Package Optical I/O," IEEE Micro, 40:2, 63-71, Mar 2020.